Internal friction measurements of low energy excitations in amorphous germanium thin films

Thomas H. Metcalf[a,*], Xiao Liu[a], Glenn Jernigan[b], James C. Culbertson[b], Matthew Abernathy[c,1], Manel Molina-Ruiz[d], Frances Hellman[d]

[a] *Naval Research Laboratory Code 7130, Washington DC, 20375, USA*
[b] *Naval Research Laboratory Code 6800, Washington DC, 20375, USA*
[c] *NRC Postdoctoral Associate, Washington DC, 20375, USA*
[d] *Department of Physics, University of California Berkeley, Berkeley CA 94720, USA*

Abstract

Motivated to create a germanium analog to nearly two-level-tunneling-system (TLS)-free amorphous silicon, six germanium films, all about 350 nm thick, were deposited by molecular beam epitaxy onto substrates held at temperatures between room temperature and 280°C. The internal friction and speed of sound of the films was measured between 375 mK and 300 K. Although the intent was to study amorphous thin films, those grown at 200°C and higher were shown to be at least partially crystalline. The tunneling strength C, a measure of the interaction between phonons and two-level tunneling systems, decreased monotonically with increasing substrate growth temperature, and for films grown on substrates at temperatures above room temperature, C was below the glassy range. The lowest value for an amorphous film, for the 160°C-grown film, was $C = 1.9 \times 10^{-5}$.

Keywords: amorphous germanium, internal friction, two-level tunneling systems

*Corresponding author
Email address: tom.metcalf@nrl.navy.mil (Thomas H. Metcalf)
[1] Present address: The Johns Hopkins University Applied Physics Laboratory, Laurel MD, 20723, USA

1. Introduction

Since their discovery in 1971 [1], almost all amorphous dielectric materials have been shown to have low-energy excitations that dominate their low-temperature thermal, acoustic, and dielectric properties, resulting in behavior markedly different from that in their crystalline counterparts, in which these excitations are typically not present. The excitations themselves, and most properties which can be ascribed to them, have been successfully, if phenomenologically, explained in the model of two-level-tunneling-systems (TLSs) [2, 3]. In this model, an individual tunneling system is an atom or group of atoms with two distinct and energetically similar spatial configurations which are separated by an energy barrier that, although insurmountable at low temperatures by thermal activation, has a nonzero tunneling probability. The TLSs couple to the strain field, scattering phonons via both resonant and relaxational processes. The TLS model calculations show that a broad distribution of TLSs in both energy and relaxation time reproduces many of the experimentally observed phenomena.

A remarkable aspect seen in TLS measurements has been universality: over the entire broad swath of amorphous materials that have been studied, the concentration of TLSs, by various measures, changes very little. This universality is not predicted by the TLS theory. The inability to substantially modify the TLS concentration has made identification of the microscopic nature of TLSs elusive.

Shortly after this theory was proposed, it was suggested that TLSs would be fewer in number, or altogether nonexistent, in four-fold-coordinated amorphous systems, in which the atomic networks could be overconstrained in a way that inhibited the formation of TLSs [3, 4]. The most apparent candidates for TLS-free amorphous dielectrics were amorphous silicon and germanium, and in the subsequent decades, numerous experiments using with these materials produced conflicting answers, which will be discussed below. The most substantial roadblock to definitive experimental results is the fact that neither silicon nor

germanium is a glass former; their amorphous phases can not be produced by rapid cooling of a melt. As a result, *a*-Si and *a*-Ge can only be produced in a thin film form via vapor deposition, which presents a challenge for the sensitivity of the standard experimental techniques.

A significant advance came with the development of a technique optimized for the measurement of the internal friction of thin films, using a mechanical resonator known as a Double-Paddle Oscillator (DPO). Using the DPO method—also used for the present results; see Section 4—Liu, et al., measured a thin film of hydrogenated amorphous silicon that did show a dramatically lower density of TLSs than had been previously observed [5]. Further work demonstrated that *a*-Si did not always form a low-TLS configuration: the density of TLSs could be "tuned" by varying the substrate temperature during film growth [6]. In the TLS model, the tunneling strength C characterizes the interaction of phonons and TLSs; more details follow in Section 2. Overall, values for C in *a*-Si varied by nearly three orders of magnitude as the substrate temperature was increased, $1.5 \times 10^{-7} \leqslant C_{a-\mathrm{Si}} \leqslant 10^{-4}$. By contrast, values of C for nearly all other amorphous dielectric materials lie within one order of magnitude of each other, $10^{-4} \leqslant C \leqslant 10^{-3}$, an interval known as the "glassy range" [7].

Not only was it established that *a*-Si could be essentially TLS-free, but further, that the TLSs were not an inherent result of amorphicity but were sensitive in some way to the material's structure. This continuously variable concentration of TLS is a marked departure from the universality observed in other amorphous systems, which researchers have been trying to accomplish since the theory was developed. Left unresolved was the question of whether the elimination of TLSs in *a*-Si still required the overconstrained four-fold-coordinated structure, or whether the vapor deposition process could produce TLS-free amorphous dielectrics in other material systems.

In recent years, the question of whether other TLS-free amorphous dielectrics can be produced has taken on a renewed, practical interest, particularly for the development of quantum computing. It has long been known that TLSs couple to electric fields and produce dielectric loss [8], and that those individual TLSs

which are polarizable couple to both strain and electric fields [9]. In this way, TLSs have been an unexpected source of decoherence and loss in qubits based around superconducting Josephson Junctions [10, 11].

Given the success of TLS reduction in a-Si, it is natural to look to germanium for a similar TLS-free amorphous solid, as they share the four-fold coordination and are chemically very similar. To this end we undertook the present work. Germanium films were deposited onto substrates spanning a wide temperature range, and their TLS density was measured with the DPO method of low temperature internal friction.

2. TLS model

An individual TLS is characterized by an asymmetry ϵ and a wavefunction overlap λ. The TLS model presumes that the spectral density of tunneling states, $P(\epsilon, \lambda) = \bar{P}$, in units per unit energy per unit volume, is constant over a broad range of ϵ and λ. Introducing the coupling energy γ of phonons to the TLSs, we get a dimensionless parameter known as the tunneling strength

$$C = \frac{\bar{P}\gamma^2}{\rho v^2} \tag{1}$$

where ρ is the material density and v is the speed of sound. The tunneling strength can be measured from thermal conductivity or internal friction measurements [7]. When resonant scattering of TLSs is the dominant phonon scattering mechanism in an amorphous solid, the thermal conductivity at low temperatures shows a T^2 dependence and C can be extracted from the prefactor if the speed of sound is known. But in thin films particularly, other phonon scattering mechanisms can compete in the overall scattering and obscure the TLS contribution.

Internal friction is most commonly associated with the oscillating strain field of a mechanical resonator. Associated with any resonator are several simultaneously acting energy loss mechanisms; those which are intrinsic to the material itself constitute internal friction. Internal friction is measured as an inverse quality factor Q^{-1} measuring the fraction of energy lost per oscillation cycle to

these internal processes. The relaxation interaction of TLS with an oscillating strain field produces a T^3 internal friction at very low temperatures, and above 10 K, the internal friction tends to be dominated by thermally activated processes [12, 13]. But for $0.1\,\mathrm{K} \lesssim T \lesssim 10\,\mathrm{K}$, a range where TLS relaxation is very fast compared to resonator oscillation frequencies, TLS result in a temperature-independent internal friction plateau. The internal friction in this plateau range, Q_0^{-1}, is related to the tunneling strength by:

$$Q_0^{-1} = \frac{\pi}{2} C. \tag{2}$$

3. Previous measurements on *a*-Ge

The question of TLS in *a*-Ge has been investigated by several experimental techniques, the results of which have been inconsistent.

As low-energy excitations with a broad and flat energy distribution, TLSs have a specific heat that increases linearly with temperature T. This contribution is in addition to the usual Debye T^3 specific heat, and for $T \leqslant 1\,\mathrm{K}$, the linear term from TLSs is larger and dominates the total specific heat. But while measurements on *a*-Ge have found heat capacity in excess of the Debye contribution, it has been attributed to sources other than TLSs. King, Phillips, and deNeufville measured the heat capacity of a room-temperature sputtered 20 μm *a*-Ge film between 2 K and 30 K, [14] and found that any linear term in the heat capacity would need to be smaller than that observed in other glassy materials. Löhneysen and Schink measured the heat capacity of three *a*-Ge films deposited by electron beam evaporation at less than 100°C, and found both an excess T^3 contribution (compared to *c*-Ge) and contributions in addition to that [15, 16]. But the linear term was at least 6× lower than that for silica, did not extend past 0.4 K, and was reduced by annealing at 350°C. The excess specific heat was attributed to exchange-coupled clusters of unpaired electrons instead of TLS. Further measurements showed a linear component to the heat capacity vanishing in a 6 T magnetic field; TLS contributions should not be magnetic-field dependent [17].

By contrast, thermal conductivity measurements have shown evidence for TLS in *a*-Ge. Measurements of 2–6 μm *a*-Ge films by von Löhneysen showed both a plateau range and a temperature dependence consistent with TLS-dominated glassy behavior [18]. More controversial measurements were made by Graebner [19, 20], who deposited, using thermal evaporation, *a*-Ge films slightly thicker than 10 μm onto a substrate held at temperatures between 25°C and 130°C. The quantity $\bar{P}M^2$, equivalent to $\bar{P}\gamma^2$ from Eq. (1), was extracted via a 6-parameter fit. The density of each film was measured and values of $\bar{P}M^2$ decreased with increasing density. This work was criticized on the grounds that phonon scattering by TLSs in thin films would be smaller than that attributable to boundary or Rayleigh scattering, such that the extraction of any TLS parameters would need to presume the existence of TLSs in the first place [21].

Surface acoustic wave measurements, the method most closely related to the internal friction measurements that will be presented below, have produced conflicting results for *a*-Ge. Bhatia, *et al.*, measured 0.3 μm [22] *a*-Ge and *a*-Ge:H films between 0.5 K and 475 K, and later measured an 0.5 μm *a*-Ge film [23] between 0.45 K and 300 K. The films were sputter-deposited and the measurements were conducted at 300 MHz. The temperature dependence of neither the attenuation nor the speed of sound showed any characteristics of TLS. Duquesne and Bellessa sputter-deposited a much thicker 20 μm *a*-Ge film onto a substrate held at 180°C and measured it between 0.1 K and 10 K at 24, 110, and 200 MHz [24, 21]. With a penetration depth of about 15 μm, the highest-frequency wave propagated entirely within the film and thus probed the variation of speed of sound of the film, which was found to increase with increasing temperature following a logarithmic law indicative of resonant interaction with TLS. After annealing at 350°C, this behavior persisted at approximately the same magnitude. It was concluded that their *a*-Ge does have TLSs, but at a value of $\bar{P}B_R^2$ a factor of 13 smaller than in a typical amorphous solid, where the deformation potential B_R is comparable to γ. This gives $C \approx 2.4 \times 10^{-5}$.

In the course of work on *a*-Si, Liu, Pohl, and Crandall have measured the internal friction of four *a*-Ge films using the DPO method [25, 26, 27]. Two 500 nm

thick films were deposited below 100°C, one sputtered, and one e-beam evaporated, and two hydrogenated a-Ge films were deposited at 330°C using hot-wire chemical vapor deposition (HWCVD), one 2.1 μm and the other 540 nm. The e-beam and sputtered films had nearly identical internal friction, each with a broad, flat plateau below 10 K, just below the glassy range, while the two hydrogenated films had substantially lower internal friction below 10 K, giving $C \approx 3 \times 10^{-6}$, well below the glassy range but still indicating the presence of some TLSs. These results will be discussed in more detail below.

4. Experimental

We measure internal friction with the Double-Paddle Oscillator (DPO) method [28, 29]. The DPO is a macroscopic mechanical resonator fabricated from single-crystal silicon wafers using conventional microfabrication techniques. The DPOs used in this work are fabricated from 300 μm-thick $\langle 1\,0\,0 \rangle$-oriented wafers and have overall planar dimensions of 19.6 mm by 28.2 mm. The outline of the DPO is shown in inset (a) to Fig. 1.

The DPOs have a metal film evaporated onto the foot, leg, and part of the wings which acts as an electrode for capacitive excitation. To measure, a DPO is clamped in an Invar mounting block and secured to a sample holder that brings drive and detection electrodes to within 0.5 mm of the metal film. This is all sealed in the vacuum can of a ^{3}He cryostat, in which measurements are carried out between 375 mK and 300 K.

We excite the DPO into its ninth resonance mode, an anti-symmetric torsional resonance in which the head and wings vibrate 180° out of phase, twisting the neck. This mode is the second such anti-symmetric torsional mode, and is termed "AS2." AS2 is illustrated in inset (b) of Fig. 1. It has a resonant frequency of approximately 5500 Hz and at low ($T < 30$ K) temperatures, a very low damping, $Q^{-1} < 2 \times 10^{-8}$. (Above 30 K, Q^{-1} of a bare DPO is dominated by thermoelastic damping [30].) Here, Q is the dimensionless quality factor of the resonator, which is measured from the free ringdown decay of the resonator's

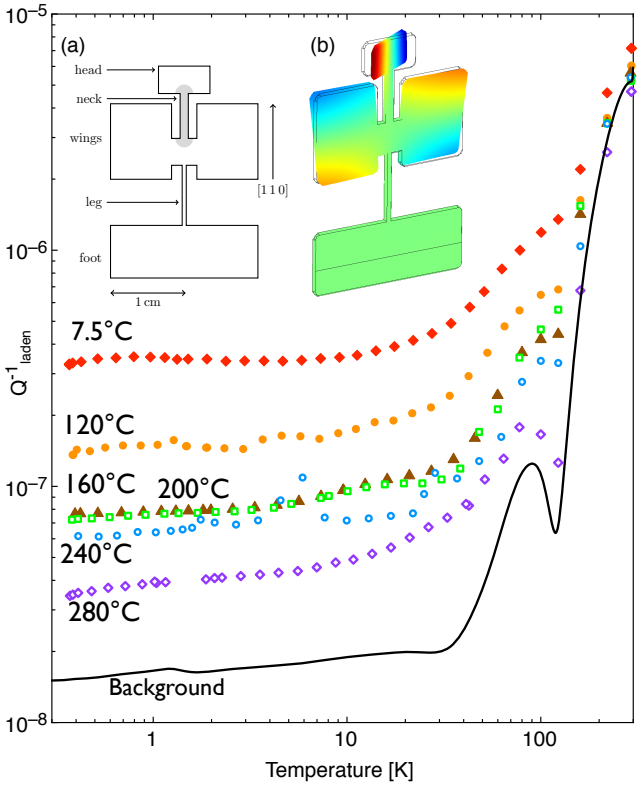

Figure 1: Inset (a): Outline of DPO. Shaded region shows area where film is deposited. Inset (b): FEM computation of AS2 deflection. Color scale represents out-of-plane deflection. Main figure: $Q^{-1}_{\rm laden}$ versus Temperature (symbols) for the samples measured in this work, together with representative $Q^{-1}_{\rm bare}$ (solid line). Here, amorphous germanium films are shown by solid symbols, partially crystallized films by open symbols. Solid red diamonds: 7.5°C (room temperature); solid orange circles: 120°C; solid brown triangles: 160°C; green open squares: 200°C; blue open circles: 240°C; purple open diamonds: 280°C.

amplitude. The background Q^{-1}, together with the data to be discussed below, is shown in Fig. 1.

Considering the DPO as a lumped element damped harmonic resonator, the geometry is such that for AS2, the first-order, lump-sum inertial term is given by the moment of inertia of the head, while the restoring force is determined by the torsion constant of the neck. Thus a film that is deposited only on the neck of the DPO will change only the restoring force and not the inertial term, so that the frequency shift is directly proportional to the film's shear modulus,

with no contribution from mass loading. The changes of the frequency f_{bare} and damping Q^{-1}_{bare} of a bare DPO to f_{laden} and Q^{-1}_{laden} of a film-laden DPO upon deposition of a film are described by:

$$\frac{f_{\text{laden}} - f_{\text{bare}}}{f_{\text{bare}}} = \frac{\Delta f}{f} = \frac{3G_{\text{film}}t_{\text{film}}}{2G_{\text{sub}}t_{\text{sub}}} \tag{3}$$

$$Q^{-1}_{\text{laden}} = \frac{3G_{\text{film}}t_{\text{film}}}{G_{\text{sub}}t_{\text{sub}}}Q^{-1}_{\text{film}} + Q^{-1}_{\text{bare}} \tag{4}$$

$$= 2\frac{\Delta f}{f}Q^{-1}_{\text{film}} + Q^{-1}_{\text{bare}} \tag{5}$$

Where the "t"s are thicknesses, G_{film} is the shear modulus of the film, and $G_{\text{sub}} = 62\,\text{GPa}$ is the shear modulus of the silicon DPO substrate about the $\langle 1\,1\,0\rangle$ axis of the neck. Calculating G_{film} and Q^{-1}_{film} is a matter of inverting Eqs. (3) and (5). Note that although we measure G_{film} if we know t_{film}, we get the product $G_{\text{film}}t_{\text{film}}$ from the frequency shift, so the Q^{-1}_{film} measurement is not affected by uncertainty in t_{film}.

The utility of the DPO for thin film measurements, especially compared with other TLS measurements such as thermal conductivity or specific heat, can be illustrated by considering a 1 nm film of a typical glass. If $Q^{-1}_{\text{film}} = 5 \times 10^{-4}$ and the film has a shear modulus comparable to that of silicon, Eq. (5) yields a change $\Delta Q^{-1} \approx 5 \times 10^{-9} \approx 0.25\,Q^{-1}_{\text{bare}}$, a clear and strong signal.

The DPO provides an additional measure of the TLS through the variation in film speed of sound [31]. In the same temperature region, if $v_0 = v_{\text{film}}(T_0)$, for an (arbitrary) reference temperature T_0, then [32]

$$\frac{v - v_0}{v_0} = \frac{\Delta v}{v_0} = -\beta(T - T_0) \tag{6}$$

where β is an empirical parameter which, although not a part of the TLS formalism, has been observed to be proportional to C [33]. The variation in speed of sound is calculated from:

$$\frac{\Delta v}{v_0} = \frac{G_{\text{sub}}t_{\text{sub}}}{3G_{\text{film}}t_{\text{film}}}\left(\left.\frac{\delta f(T)}{f_0}\right|_{\text{laden}} - \left.\frac{\delta f(T)}{f_0}\right|_{\text{bare}}\right) \tag{7}$$

where $f_0 = f(T_0)$, and $\delta f(T) = f(T) - f_0$. Note that we have two distinct types of change in frequency: δf denotes changes as a function of temperature of a DPO sample measurement, while Δf denotes changes at given temperature between a DPO in its bare and film-laden states.

For this work, six germanium films, all approximately 350 nm thick, were deposited onto DPO substrates at temperatures between 7.5°C and 280°C. Depositions were done using a Ge e-beam source in a VG V80 molecular beam epitaxy (MBE) system. The MBE system is liquid nitrogen cooled, with a base pressure of $\approx 8 \times 10^{-11}$ Torr, which rises during deposition to an operating pressure of $\approx 2 \times 10^{-9}$ Torr. The Ge was evaporated at 0.05 nm/s, as measured in situ with an EIES Infocon flux deposition monitor. Substrates were heated radiatively from the backside using a 4-inch graphite heater, which is larger than the 3-inch substrate holder to assure uniform heating. Temperatures above 200°C are measured by a pyrometer that is calibrated to the observation of the eutectic points of Au/Si (363°C), and Al/Si (577°C). For temperatures below 200°C, a thermocouple embedded in the sample stage is used and similarly calibrated. The stage thermocouple consistently lags behind the pyrometer temperature due to the mass of the stage, and this is taken into account by allowing sufficient time for the stage temperature to equilibrate before deposition.

Density measurements of select films were taken using Rutherford Backscattering Spectrometry (RBS) and profilometry at UC Berkeley and are listed in Table 1. The amorphicity of the films was checked using Raman spectroscopy, the spectra are shown in Fig. 2. Although we had intended to grow six amorphous films at the successively increasing substrate temperatures, the 200, 240, and 280°C films clearly show the 300 cm^{-1} peak characteristic of crystalline germanium [34]. The crystallization of the higher-temperature films was unexpected, as silicon films grown at similar temperatures (scaled by melting point) remained amorphous.

The lower-temperature films show a broader, shorter peak centered near 280 cm^{-1} that arises from the transverse-optic (TO)-like band in amorphous germanium. In *a*-Si, higher growth temperatures led to a narrower TO-like

peak, indicating a decrease in bond-angle disorder [35]. Here, we do find that the 120°C film has a narrower peak than the 7.5°C film. Following the method of Tsu, this corresponds to bond-angle deviations decreasing from 8.3° to 7.4° [36]. The peak for the 160°C film, however, is wider. Inspection of the curve in Fig. 2 shows a steep drop near 300 cm^{-1} that could indicate the beginnings of a crystallization peak superimposed upon the broad amorphous peak.

5. Results and Discussion

The raw Q^{-1}_{laden} measurements are shown in Fig. 1. Also shown is a typical Q^{-1}_{bare} measurement; all Q^{-1}_{bare} measurements for this work are within 10% of the curve shown. The presence of the films increases the Q^{-1} of the DPO by a factor between 2 and 20. The Q^{-1}_{laden} measurements are flat and featureless, rising gradually above 30 K as Q^{-1}_{bare} rises as well. It has been shown that TLSs exist in both amorphous and crystalline phases of partially crystallized materials, but their density and origin in the crystalline phase is unknown [37, 7]. Thus despite the crystallization, we consider the TLS measurements on the 200°C+ films to provide useful information. We note the form of Q^{-1}_{laden} versus temperature is the same for the partially crystallized as for the amorphous films; the crystallization doesn't appear to have introduced any additional energy loss mechanisms. We will treat C values as representative of the entire film, including the crystallized regions.

From the data shown in Fig. 1, Q^{-1}_{film} values are calculated using Eq. (2). The low-temperature plateau values for each film, Q_0^{-1}, then gives C through Eq. (1). Values of C are shown as a function of substrate deposition temperature in Fig. 3, and the $\Delta v/v$ versus temperature data are shown in Fig. 4. A summary of the data is given in Table 1. Values for C and β decrease with increasing substrate temperature. The value of C for the 7.5°C-grown sample lies at the lower edge of the glassy range, while values for all of the films grown at higher temperatures are below the glassy range. However, even the highest-temperature-grown (280°C), partially crystallized film doesn't reach the low C

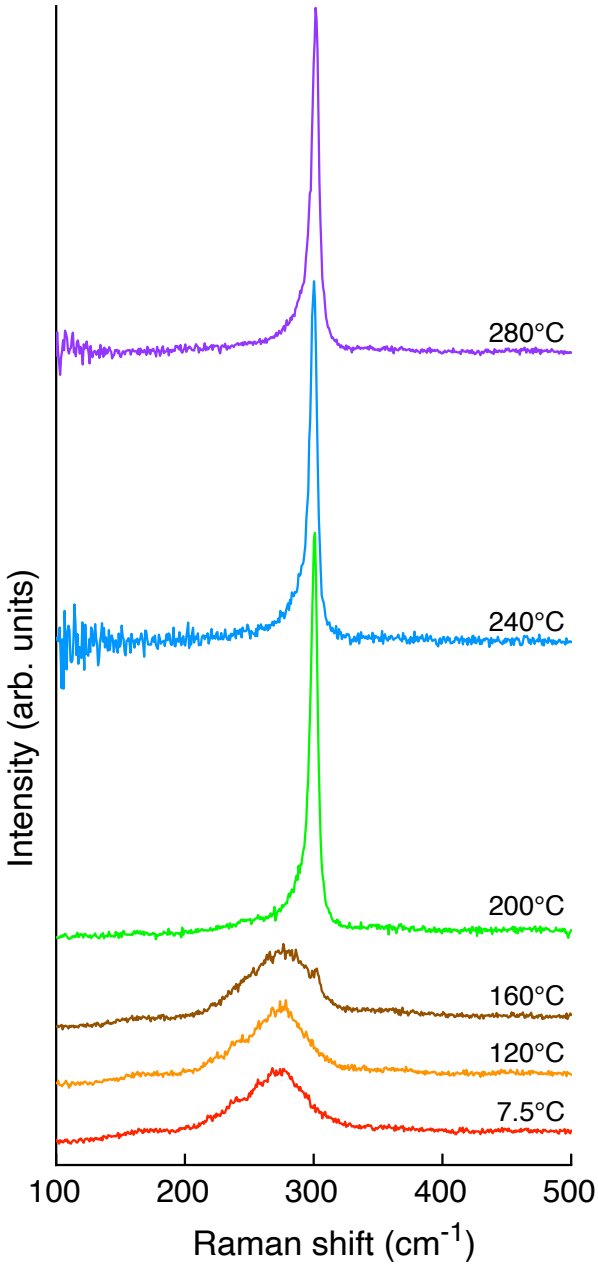

Figure 2: Raman spectra for the germanium films studied in this work. Color scheme is the same as Fig. 1. Individual curves are normalized to have the same integrated area and are offset for clarity.

Present data

T (°C)	X/A	thickness (nm)	density 10^{22} at/cm^3	density g/cm^3	Q_0^{-1}	C	β $\times 10^{-6}$	$G_{\rm film}$ GPa
7.5	A	350.9	3.91	4.72	1.82×10^{-4}	1.16×10^{-4}	37.2	31.14
120	A	334.4	4.13	4.98	6.70×10^{-5}	4.26×10^{-5}	16.3	36.5
160	A	343.4	4.28	5.16	2.93×10^{-5}	1.87×10^{-5}	12.4	38.63
200	X	392.0	4.39	5.29	2.11×10^{-5}	1.34×10^{-5}	9.76	42.29
240	X	389.5			1.56×10^{-5}	9.93×10^{-6}	5.00	47.3
280	X	324.4			9.50×10^{-6}	6.05×10^{-6}	2.32	50.98

Table 1: Specifications of films measured in this work. 'X' indicates a crystalline film; 'A' amorphous.

values found for a-Si. Values for $\Delta v/v_0$ show the linear temperature dependence characteristic of amorphous solids, with the absolute value of the slope decreasing with increasing deposition temperature. This speed of sound data is consistent across the amorphous and partially crystalline films.

Also shown in Fig. 3 are values from four a-Ge films from Liu, Pohl, and Crandall that were discussed in Section 3. Their parameters are summarized in Table 2. The e-beam deposited and the sputtered films, both deposited at temperatures below 100°C, have notably lower C values than our 7.5°C film and are close in magnitude to that of the present 120°C-deposited film. The HWCVD films, despite being grown at a substrate temperature of 330°C, have been verified to be amorphous. These a-Ge:H films have $C < 4\times10^{-6}$. Note that $G_{\rm film}$ was not independently measured for any of these films; in the technology of the time the bare DPO could not be measured prior to film deposition. From the uncertainty both in $Q_{\rm bare}^{-1}$ and $G_{\rm film}$ we estimate each of these C values to have 20% uncertainties.

The current thinking around TLS reduction in a-Si is that the elevated substrate temperature during film growth gives incoming adatoms sufficient mobility with which to diffuse about the surface, exploring both the physical and potential energy landscapes of the growing film. These atoms are then able to settle in low energy configurations before their surface diffusive motion is constrained by the accumulation of subsequent film layers. These lower energy

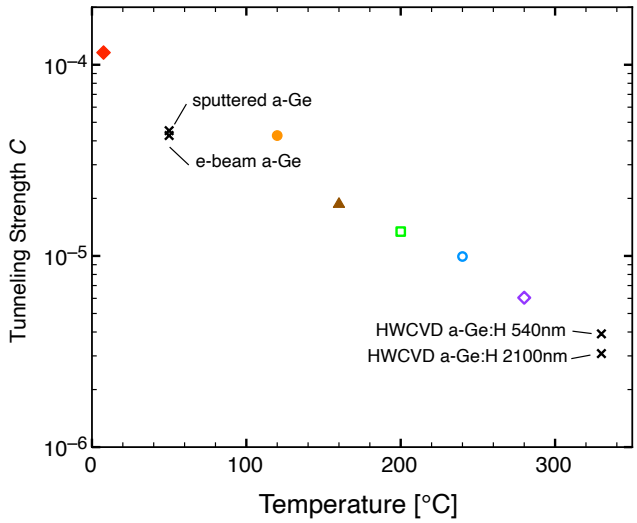

Figure 3: C versus substrate temperature during film growth. Symbols for present data are the same as in Fig. 1: solid symbols are amorphous films, open symbols are partially crystalline. Also shown as × symbols are previous DPO measurements on a-Ge films from Ref. [25] and a-Ge:H films from Ref. [27], all of which are listed in Table 2.

Previous DPO data

Source	preparation	T_s °C	t nm	Q_0^{-1}	C	β	$G_{\rm film}$ GPa
[25]	ebeam	$\leqslant 100$	500	6.7×10^{-5}	4.3×10^{-5}	1.37×10^{-5}	29
[25]	sputtered	$\leqslant 100$	500	7.1×10^{-5}	4.5×10^{-5}	5.69×10^{-6}	16
[27]	HWCVD a-Ge:H	330	2100	4.84×10^{-6}	3.08×10^{-6}		39
[27]	HWCVD a-Ge:H	330	540	6.13×10^{-6}	3.90×10^{-6}		39

Table 2: Specifications of previously published a-Ge films measured with the DPO technique. $G_{\rm film}$ are the presumed values, taken from literature, used in the analysis. The substrate temperature for the e-beam film was "kept below 100°C by water cooling."

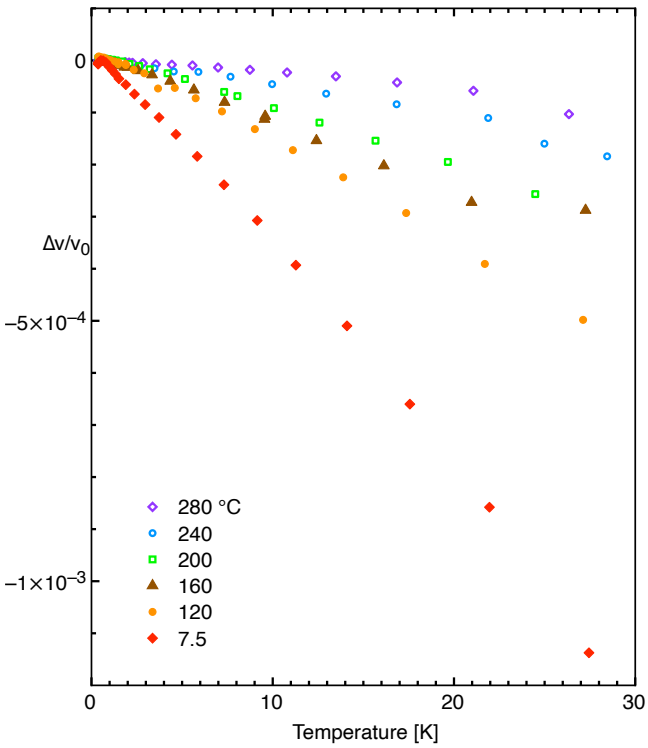

Figure 4: $\Delta v/v_0$ versus Temperature for the six films measured in this work. Legend indicates film substrate growth temperature.

configurations, in turn, are less likely to be the locus of a TLS. This process is at least an analog to that described for ultrastable organic glasses, where vapor deposition at 85% of a material's glass transition temperature can lead to a glass with exceptional kinetic stability when compared to a liquid-quenched glass of the same chemical composition [38, 39]. It has been further suggested that ultrastable glasses have reduced TLS compared to their liquid-quenched counterparts, as has been observed in a measurement of the specific heat of vapor-deposited indomethacin [40]. The arrangement of incoming atoms in a generally lower energy configuration will also result in a denser material. It has been observed in *a*-Si that the density of TLSs decreases exponentially with increasing atomic density [35, 41]. We find the same trend in these *a*-Ge data, as shown in Fig. 5. This supports the notion of TLSs formed in local regions of low density that are relatively high energy configurations.

Also shown in Fig. 5 are data from Graebner [19], which were extracted from a six-parameter fit to thermal conductivity data. Given the dubious validity of this procedure, the agreement with our measurements is remarkable. However, while our data suggest a purely exponential decrease of C with increasing density, Graebner's data suggests a stronger than exponential decay.

The crystallization of the 200°C+ films is somewhat unexpected: thermally evaporated germanium films have remained amorphous at higher substrate temperatures than for the present films. One study has found that partial crystallization begins at 240°C with full crystallization happening between 250°C and 285°C, depending on the substrate, [42] and in others, germanium films have remained amorphous when deposited onto substrates held at 300°C [43, 44]. The HWCVD *a*-Ge:H films shown above remained amorphous at 330°C. A comparison with silicon suggests that germanium crystallizes more readily: 200°C, the lowest temperature for a partially crystallized Ge film, is 39% of the melting point of germanium, while the deposition of *a*-Si films in earlier work [6] at 400°C, which is 40% of the melting point, remained amorphous, with no crystallization appearing until 450°C, 43% of the melting point.

If impurities inhibit crystallization, the ultra-high vacuum conditions in our

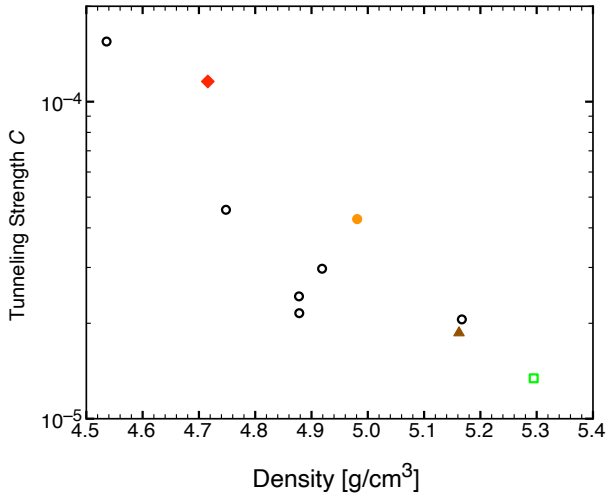

Figure 5: Values of C as a function of mass density of films. Symbols for present data same as Fig. 1; open circles (○) are data from Graebner [19].

deposition system may induce crystallization at comparatively low temperatures. Germain, Zellema, et al., measured the Gibbs energy for migration—the barrier for an atom to jump from the amorphous to the crystalline phase—in *a*-Ge [45] and *a*-Si [46]. The values for germanium are lower, approximately 63% of that of silicon in the temperature range of our depositions. Additionally, the germanium atom is 10% larger than the silicon atom, and this combined with weaker bonding may make germanium more likely to reorient than to diffuse.

We do note that the *a*-Ge:H films published earlier and included in Fig. 3 have lower Q_0^{-1}, and lower C, than even the highest-temperature, partially crystalline film from the present study. This is also the case for *a*-Si: the lowest $C_{a\text{-Si}} = 1.6 \times 10^{-7}$ that has been reported is for an HWCVD *a*-Si:H film labeled "HW14," [26] which is lower than $C_{400^\circ\text{C}} = 1.3 \times 10^{-6}$ for the 400°C grown *a*-Si film from Liu [6]. This could either indicate the importance of hydrogen incorporation, or it could be an indication that the HWCVD method inherently produces lower-energy configuration films than the present method.

6. Conclusions

In a sense, the prior literature was asking the wrong question. The question is not "does amorphous germanium have two-level tunneling systems?" because this question presumes that all amorphous germanium is essentially the same, and that the different experimental answers to that question were the result of insufficient experimental sensitivity or sample contamination. By showing that amorphous germanium can have a variable density of TLSs, it is clear that a more appropriate question is "what growth parameters reduce the density of TLSs in amorphous germanium?" and "how low can the density of TLSs get in amorphous germanium?" As in *a*-Si, elevated substrate temperature does reduce TLS, but the goal of low-TLS *a*-Ge in the present work was confounded by crystallization. The aim of the elevated substrate temperature deposition is to give the incoming adatoms enough energy to find a low-energy configuration, but not so much energy that they crystallize. Finding a way to keep this balance at substrate temperatures of 200°C and above is a challenge for future work.

7. Acknowledgements

This work supported by the Office of Naval Research. MMR and FH acknowledge support from NSF through award DMR-1809498.

References

[1] R. Zeller, R. Pohl, Thermal conductivity and specific heat of noncrystalline solids, Phys. Rev. B 4 (1971) 2029–2041. doi:10.1103/PhysRevB.4.2029.
URL https://doi.org/10.1103/PhysRevB.4.2029

[2] P. W. Anderson, B. I. Halperin, C. M. Varma, Anomalous low-temperature thermal properties of glasses and spin glasses, Philos. Mag. A 25 (1) (1972) 1–9. doi:10.1080/14786437208229210.
URL https://doi.org/10.1080/14786437208229210

[3] W. A. Phillips, Tunneling states in amorphous solids, J. Low Temp. Phys. 7 (3) (1972) 351–360. doi:10.1007/BF00660072.
URL https://doi.org/10.1007/BF00660072

[4] M. Von Haumeder, U. Strom, S. Hunklinger, Acoustic anomalies in amorphous thin films of Si and SiO_2, Phys. Rev. Lett. 44 (1980) 84–87. doi:10.1103/PhysRevLett.44.84.
URL https://link.aps.org/doi/10.1103/PhysRevLett.44.84

[5] X. Liu, B. E. White, Jr., R. O. Pohl, E. Iwanizcko, K. M. Jones, A. H. Mahan, B. N. Nelson, R. S. Crandall, S. Veprek, Amorphous solid without low energy excitations, Phys. Rev. Lett. 78 (23) (1997). doi:10.1103/PhysRevLett.78.4418.
URL http://link.aps.org/doi/10.1103/PhysRevLett.78.4418

[6] X. Liu, D. R. Queen, T. H. Metcalf, J. E. Karel, F. Hellman, Hydrogen-free amorphous silicon with no tunneling states, Phys. Rev. Lett. 113 (2014) 025503. doi:10.1103/PhysRevLett.113.025503.
URL https://link.aps.org/doi/10.1103/PhysRevLett.113.025503

[7] R. O. Pohl, X. Liu, E. Thompson, Low-temperature thermal conductivity and acoustic attenuation in amorphous solids, Rev. Mod. Phys. 74 (2002) 991–1013. doi:10.1103/RevModPhys.74.991.
URL https://doi.org/10.1103/RevModPhys.74.991

[8] M. von Schickfus, S. Hunklinger, L. Piché, Anomalous dielectric dispersion in glasses at low temperatures, Phys. Rev. Lett. 35 (1975) 876–878. doi:10.1103/PhysRevLett.35.876.
URL https://link.aps.org/doi/10.1103/PhysRevLett.35.876

[9] C. Laermans, W. Arnold, S. Hunklinger, Influence of an electromagnetic wave on the acoustic absorption of borosilicate glass at low temperatures, J. Phys. C 10 (8) (1977) L161–L165. doi:10.1088/0022-3719/10/8/001.
URL https://doi.org/10.1088/0022-3719/10/8/001

[10] R. W. Simmonds, K. M. Lang, D. A. Hite, S. Nam, D. P. Pappas, J. M. Martinis, Decoherence in josephson phase qubits from junction resonators, Phys. Rev. Lett. 93 (2004) 077003. doi:10.1103/PhysRevLett.93.077003.
URL https://link.aps.org/doi/10.1103/PhysRevLett.93.077003

[11] J. M. Martinis, K. B. Cooper, R. McDermott, M. Steffen, M. Ansmann, K. D. Osborn, K. Cicak, S. Oh, D. P. Pappas, R. W. Simmonds, C. C. Yu, Decoherence in josephson qubits from dielectric loss, Phys. Rev. Lett. 95 (2005) 210503. doi:10.1103/PhysRevLett.95.210503.
URL https://link.aps.org/doi/10.1103/PhysRevLett.95.210503

[12] A. K. Raychaudhuri, S. Hunklinger, Low frequency elastic properties of glasses at low temperatures—implications on the tunneling model, Z. Phys. B V57 (2) (1984) 113–125. doi:10.1007/BF02071961.
URL http://dx.doi.org/10.1007/BF02071961

[13] K. A. Topp, D. G. Cahill, Elastic properties of several amorphous solids and disordered crystals below 100K, Z. Phys. B V101 (2) (1996) 235–245. doi:10.1007/s002570050205.
URL http://dx.doi.org/10.1007/s002570050205

[14] C. N. King, W. A. Phillips, J. P. deNeufville, Low-temperature heat capacity of amorphous germanium, Phys. Rev. Lett. 32 (1974) 538–541. doi:10.1103/PhysRevLett.32.538.
URL https://link.aps.org/doi/10.1103/PhysRevLett.32.538

[15] H. v. Löhneysen, H. J. Schink, Specific heat of amorphous germanium at very low temperatures, Phys. Rev. Lett. 48 (1982) 1121–1124. doi:10.1103/PhysRevLett.48.1121.
URL https://link.aps.org/doi/10.1103/PhysRevLett.48.1121

[16] H. von Löhneysen, Specific heat of amorphous Ge and Si at very low temperatures, J. Non-Cryst. Solids 59-60 (1983) 1087 – 1094, proceedings

of the Tenth International Conference on Amorphous and Liquid Semiconductors. doi:10.1016/0022-3093(83)90356-3.
URL http://www.sciencedirect.com/science/article/pii/0022309383903563

[17] R. van den Berg, H. v. Löhneysen, Magnetic excitations in amorphous germanium studied by high-field calorimetry, Phys. Rev. Lett. 55 (1985) 2463–2466. doi:10.1103/PhysRevLett.55.2463.
URL https://link.aps.org/doi/10.1103/PhysRevLett.55.2463

[18] H. v. Löhneysen, F. Steglich, Low-temperature thermal conductivity of amorphous germanium, Phys. Rev. Lett. 39 (1977) 1420–1423. doi:10.1103/PhysRevLett.39.1420.
URL https://link.aps.org/doi/10.1103/PhysRevLett.39.1420

[19] J. E. Graebner, L. C. Allen, Tunneling systems in amorphous germanium, Phys. Rev. Lett. 51 (1983) 1566–1569. doi:10.1103/PhysRevLett.51.1566.
URL https://link.aps.org/doi/10.1103/PhysRevLett.51.1566

[20] J. E. Graebner, B. Golding, L. C. Allen, J. C. Knights, D. K. Biegelsen, Thermal properties of $a-$Si:H at low temperatures, Phys. Rev. B 29 (1984) 3744–3746. doi:10.1103/PhysRevB.29.3744.
URL https://link.aps.org/doi/10.1103/PhysRevB.29.3744

[21] J. Y. Duquesne, G. Bellessa, Ultrasonic study of tunnelling defects in amorphous Se, Ge and Se–Ge compounds, Philos. Mag. B 52 (4) (1985) 821–842. doi:10.1080/13642818508238929.
URL https://doi.org/10.1080/13642818508238929

[22] K. L. Bhatia, M. v. Haumeder, S. Hunklinger, Interaction of ultrasonic phonons with defects in hydrogenated amorphous germanium, Z. Phys. B 44 (3) (1981) 155–158. doi:10.1007/BF01297170.
URL https://doi.org/10.1007/BF01297170

[23] K. Bhatia, S. Hunklinger, Effects of oxygen on the ultrasonic properties of amorphous germanium, Solid State Commun. 47 (6) (1983) 489 – 492.

doi:10.1016/0038-1098(83)91074-8.
URL http://www.sciencedirect.com/science/article/pii/0038109883910748

[24] J. Y. Duquesne, G. Bellessa, Rayleigh waves in amorphous germanium at low temperature: evidence for the existence of tunnelling defects, J. Phys. C 16 (3) (1983) L65. doi:10.1088/0022-3719/16/3/003.
URL http://stacks.iop.org/0022-3719/16/i=3/a=003

[25] X. Liu, R. O. Pohl, Low-energy excitations in amorphous films of silicon and germanium, Phys. Rev. B 58 (1998) 9067–9081. doi:10.1103/PhysRevB.58.9067.
URL https://link.aps.org/doi/10.1103/PhysRevB.58.9067

[26] R. S. Crandall, X. Liu, Elastic properties of amorphous and nanocrystalline silicon, Thin Solid Films 395 (1) (2001) 78 – 83. doi:10.1016/S0040-6090(01)01212-3.
URL http://www.sciencedirect.com/science/article/pii/S0040609001012123

[27] X. Liu, D. M. Photiadis, H.-D. Wu, D. B. Chrisey, R. O. Pohl, R. S. Crandall, Disorder in tetrahedrally bonded amorphous solids, Philos. Mag. B 82 (2) (2002) 185–195. doi:10.1080/13642810208208541.
URL http://www.tandfonline.com/doi/abs/10.1080/13642810208208541

[28] X. Liu, S. F. Morse, J. F. Vignola, D. M. Photiadis, A. Sarkissian, M. H. Marcus, B. H. Houston, On the modes and loss mechanisms of a high Q mechanical oscillator, Appl. Phys. Lett. 78 (10) (2001) 1346–1348. doi:10.1063/1.1350599.
URL https://doi.org/10.1063/1.1350599

[29] C. L. Spiel, R. O. Pohl, A. T. Zehnder, Normal modes of a Si(100) double-paddle oscillator, Rev. Sci. Inst. 72 (2001) 1482. doi:10.1063/1.1340559.
URL https://doi.org/10.1063/1.1340559

[30] D. M. Photiadis, B. H. Houston, X. Liu, J. A. Bucaro, M. H. Marcus, Thermoelastic loss observed in a high Q mechanical oscillator, Physica B

316-317 (2002) 408–410. doi:10.1016/S0921-4526(02)00528-8.
URL https://doi.org/10.1016/S0921-4526(02)00528-8

[31] G. Bellessa, Frequency and temperature dependence of the sound velocity in amorphous materials at low temperatures, Phys. Rev. Lett. 40 (1978) 1456–1459. doi:10.1103/PhysRevLett.40.1456.
URL https://link.aps.org/doi/10.1103/PhysRevLett.40.1456

[32] P. Medwick, J. B.E White, R. Pohl, Elastic properties of amorphous and crystalline $B_{1-x}C_x$ and boron at low temperatures, J. Alloys Compd. 270 (1) (1998) 1–15. doi:10.1016/S0925-8388(98)00119-4.
URL http://www.sciencedirect.com/science/article/pii/S0925838898001194

[33] B. E. White, R. O. Pohl, Elastic properties of amorphous solids below 100K, Z. Phys. B 100 (3) (1997) 401–408. doi:10.1007/s002570050139.
URL https://doi.org/10.1007/s002570050139

[34] D. Bermejo, M. Cardona, Raman scattering in pure and hydrogenated amorphous germanium and silicon, J. Non-Cryst. Solids 32 (1) (1979) 405 – 419. doi:https://doi.org/10.1016/0022-3093(79)90085-1.
URL http://www.sciencedirect.com/science/article/pii/0022309379900851

[35] D. R. Queen, X. Liu, J. Karel, T. H. Metcalf, F. Hellman, Excess specific heat in evaporated amorphous silicon, Phys. Rev. Lett. 110 (2013) 135901. doi:10.1103/PhysRevLett.110.135901.
URL https://link.aps.org/doi/10.1103/PhysRevLett.110.135901

[36] R. Tsu, J. Hernandez, F. Pollak, Determination of energy barrier for structural relaxation in a-Si and a-Ge by raman scattering, J. Non-Cryst. Solids 66 (1) (1984) 109 – 114. doi:https://doi.org/10.1016/0022-3093(84)90307-7.
URL http://www.sciencedirect.com/science/article/pii/0022309384903077

[37] A. Leadbetter, A. Jeapes, C. Waterfield, K. Wycherley, The low temperature heat capacity of some glass ceramics, Chem. Phys. Lett. 52 (3) (1977)

469 – 472. doi:https://doi.org/10.1016/0009-2614(77)80487-9.
URL http://www.sciencedirect.com/science/article/pii/0009261477804879

[38] S. F. Swallen, K. L. Kearns, M. K. Mapes, Y. S. Kim, R. J. McMahon, M. D. Ediger, T. Wu, L. Yu, S. Satija, Organic glasses with exceptional thermodynamic and kinetic stability, Science 315 (5810) (2007) 353–356. arXiv:https://science.sciencemag.org/content/315/5810/353.full.pdf, doi:10.1126/science.1135795.
URL https://science.sciencemag.org/content/315/5810/353

[39] M. D. Ediger, Perspective: Highly stable vapor-deposited glasses, J. Chem. Phys. 147 (21) (2017) 210901. doi:10.1063/1.5006265.
URL https://doi.org/10.1063/1.5006265

[40] T. Pérez-Castañeda, C. Rodríguez-Tinoco, J. Rodríguez-Viejo, M. A. Ramos, Suppression of tunneling two-level systems in ultrastable glasses of indomethacin, Proc. Nat. Acad. Sci. USA 111 (31) (2014) 11275. doi:10.1073/pnas.1405545111.
URL http://www.pnas.org/content/111/31/11275.abstract

[41] D. Queen, X. Liu, J. Karel, H. Jacks, T. Metcalf, F. Hellman, Two-level systems in evaporated amorphous silicon, J. Non-Cryst. Solids 426 (2015) 19 – 24. doi:10.1016/j.jnoncrysol.2015.06.020.
URL http://www.sciencedirect.com/science/article/pii/S0022309315300818

[42] F. Evangelisti, M. Garozzo, G. Conte, Structure of vapor - deposited Ge films as a function of substrate temperature, J. Appl. Phys. 53 (11) (1982) 7390–7396. doi:10.1063/1.330107.
URL https://doi.org/10.1063/1.330107

[43] M.-L. Theye, Influence of deposition conditions on the properties of amorphous germanium films, Opt. Commun. 2 (7) (1970) 329 – 332. doi:10.1016/0030-4018(70)90155-0.
URL http://www.sciencedirect.com/science/article/pii/0030401870901550

[44] T. Donovan, E. Ashley, W. Spicer, A high density form of amorphous Ge, Phys. Lett. A 32 (2) (1970) 85 – 86. doi:10.1016/0375-9601(70)90101-5.
URL http://www.sciencedirect.com/science/article/pii/0375960170901015

[45] P. Germain, K. Zellama, S. Squelard, J. C. Bourgoin, A. Gheorghiu, Crystallization in amorphous germanium, J. Appl. Phys. 50 (11) (1979) 6986–6994. doi:10.1063/1.325855.
URL https://doi.org/10.1063/1.325855

[46] K. Zellama, P. Germain, S. Squelard, J. C. Bourgoin, P. A. Thomas, Crystallization in amorphous silicon, Journal of Applied Physics 50 (11) (1979) 6995–7000. arXiv:https://doi.org/10.1063/1.325856, doi:10.1063/1.325856.
URL https://doi.org/10.1063/1.325856